AIAA JOURNAL
Vol. 45, No. 4, April 2007

Active Stabilization of a Hybrid Vibration Absorber Subjected to Velocity Feedback Control

M. Utsumi*
Ishikawajima-Harima Heavy Industries Company, Ltd. (IHI), Yokohama, 235-8501, Japan

DOI: 10.2514/1.17273

A method of actively stabilizing a hybrid vibration absorber driven by a force proportional to the velocity detected at the attachment position of the absorber is investigated. This method can be applied to improve model-independence of robust performance while allowing for multimode controllability for the case where a hybrid vibration absorber is desired as an actuator. Robustness not only against variations in a primary structure to be controlled but also against parameter identification errors in a vibration absorber system is discussed. It is illustrated that although this method transforms the hybrid absorber equation with a spring term into the full active absorber equation, the important advantage of a hybrid absorber over a full active absorber, that is, the power-saving effect near the first resonant frequency of a primary structure can be retained. Application examples are presented also for the vibration isolation and active noise control problems.

Nomenclature

c_a, c_{a1}, c_{a2}	=	damping constants of vibration absorbers
f_a, f_{a1}, f_{a2}	=	driving forces of vibration absorbers
f_{di}	=	disturbance force applied to the mass m_i
G	=	velocity feedback gain for the driving forces
I_i	=	inertia moment around the z axis of the ith layer (Fig. 2a)
k_a, k_{a1}, k_{a2}	=	spring constants of vibration absorbers
k_i, K_i	=	translational and rotational spring constants between the ith and $(i-1)$th layers
l_1, l_2	=	positions of vibration absorbers (Fig. 2b)
m_a, m_{a1}, m_{a2}	=	masses of vibration absorbers
m_{di}	=	disturbance moment applied to the ith layer
m_i	=	mass of the ith layer
u_a, u_{a1}, u_{a2}	=	relative displacements of masses of vibration absorbers from their attachment positions
v	=	general coordinate for masses of vibration absorbers
x_a, x_{a1}, x_{a2}	=	absolute displacements of absorber masses
x_i	=	absolute displacement of the mass m_i
α	=	damping constant of the target absorber equation
$\zeta_a, \zeta_{a1}, \zeta_{a2}$	=	damping ratios of vibration absorbers
θ_i	=	absolute rotational displacement of the ith layer (Fig. 2a)
ϕ	=	general coordinate for masses of vibration absorbers
ω	=	excitation frequency
$\omega_a, \omega_{a1}, \omega_{a2}$	=	eigenfrequencies of vibration absorbers

Introduction

A HYBRID vibration absorber has been extensively applied to control vibration of flexible structures. For widening the bandwidth where effective control performance can be achieved, a variety of methods have been developed that are characterized by a compensator that assigns selected zeros and poles to closed-loop primary systems [1], acceleration feedback with a time delay [2,3], and a feedback compensator for achieving a bandpass absorber [4]. The use of controllers designed based on modern [5,6], $H\infty$ [7,8], μ synthesis [7,8], and feedforward [9] control theory is effective for multimode control. One feature of these controllers is that they are basically model-dependent and thus their robust performance against parameter variations in the system is not so high. A promising way for achieving model-independent high robust performance is the use of adaptive-passive control technologies [10–13]. However, because these methods adjust parameters of a vibration absorber for tuning it to a target frequency, they cannot be applied to the case of broadband excitations. Thus, a method that simultaneously allows for model-independent robust performance and multimode controllability is relatively scarce for the case in which a hybrid vibration absorber is desired as an actuator due to its power-saving ability and utility as a passive element during accidents to the actuator driving system or power supply. This paper investigates such a method by considering a hybrid vibration absorber driven by a force proportional to the velocity detected at the absorber's attachment point and actively stabilizing it. Robustness not only against variations in a primary structure to be controlled but also against parameter identification errors in a vibration absorber system is discussed. Although this method transforms the hybrid absorber equation with a spring term into the full active absorber equation, this method can retain the important advantage of a hybrid absorber over a full active absorber, that is, the power-saving effect near the first resonant frequency of a primary structure. In addition to the vibration control problem, the vibration isolation problem is addressed in this paper for the case in which a damper cannot be connected to an inertial reference frame as in many practical situations. Furthermore, the present control method is extended to the active noise control problem by considering a control speaker a hybrid vibration absorber coupled with a sound field to be controlled. The active stabilization method remains important for the active noise control problem because a generally used manufactured speaker's lowest eigenfrequency is so high that it lies in the bandwidth where control is desired.

Fundamental Theory

A fundamental model as shown in Fig. 1 is considered to facilitate comprehension. Equations of motion for this model can be expressed as

$$m_1\ddot{x}_1 = -c_1\dot{x}_1 - k_1x_1 + c_a\dot{u}_a + k_au_a - f_a + f_{d1} \tag{1}$$

$$m_a\ddot{x}_a = -c_a\dot{u}_a - k_au_a + f_a \tag{2}$$

Received 24 April 2005; revision received 7 November 2006; accepted for publication 28 November 2006.

*Senior Researcher, Machine Element Department, Technical Research Laboratory, 1 Shin-Nakaharacho, Isogo-ku Yokohama, Kanagawa Prefecture 235-8501; masahiko_utsumi@ihi.co.jp.

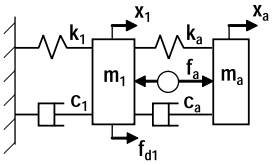

Fig. 1 Single-degree-of-freedom system with a vibration absorber.

where $u_a = x_a - x_1$. Adding Eqs. (1) and (2) to each side leads to

$$(m_1 + m_a)\ddot{x}_1 + m_a\ddot{u}_a + c_1\dot{x}_1 + k_1x_1 = f_{d1} \tag{3}$$

whereas Eq. (2) can be transformed into

$$\ddot{u}_a + 2\zeta_a\omega_a\dot{u}_a + \omega_a^2u_a = m_a^{-1}f_a - \ddot{x}_1 \tag{4}$$

where $\zeta_a = c_a/2(m_ak_a)^{1/2}$ and $\omega_a = (k_a/m_a)^{1/2}$. For the velocity feedback control $f_a = G\dot{x}_1$, the characteristic equation for Eqs. (3) and (4) is

$$a_0s^4 + a_1s^3 + a_2s^2 + a_3s + a_4 = 0 \tag{5}$$

where

$$\begin{gathered} a_0 = m_1, \qquad a_1 = (m_1 + m_a)2\zeta_a\omega_a + c_1 + G \\ a_2 = (m_1 + m_a)\omega_a^2 + 2\zeta_a\omega_ac_1 + k_1, \qquad a_3 = c_1\omega_a^2 + 2\zeta_a\omega_ak_1 \\ a_4 = k_1\omega_a^2 \end{gathered} \tag{6}$$

Because a_i $(i = 0\text{–}4)$ are positive, the remaining stability condition is that the Hurwitz determinants $D_1 \equiv a_1a_2 - a_0a_3$ and $D_2 \equiv a_3D_1 - a_4a_1^2$ are positive. For $G \to \infty$, $D_1 > 0$ is satisfied because as can be seen from Eq. (6), the gain G is contained only in a_1 and $\partial a_1/\partial G > 0$. However, $D_2 > 0$ does not admit the infinite increase of the gain G. This instability is due to the absorber resonance at the frequency ω_a.

To stabilize the control $f_a = G\dot{x}_1$, this paper determines the actuator driving force such that Eq. (4) coincides with the following target absorber equation:

$$\ddot{u}_a + \alpha\dot{u}_a = m_a^{-1}G\dot{x}_1 - \ddot{x}_1 \tag{7}$$

where α is a positive damping constant. Equation (7) can be realized by determining the driving force as

$$f_a = G\dot{x}_1 + m_a[(2\zeta_a\omega_a - \alpha)\dot{u}_a + \omega_a^2u_a] \tag{8}$$

To check the stability, we express the frequency-domain solution of Eqs. (3) and (7) as

$$\begin{Bmatrix} X_1(s) \\ U_a(s) \end{Bmatrix} = \frac{1}{a_0s^3 + a_1s^2 + a_2s + a_3} \begin{Bmatrix} s + \alpha \\ m_a^{-1}G - s \end{Bmatrix} F_{d1}(s) \tag{9}$$

where

$$\begin{gathered} a_0 = m_1, \qquad a_1 = (m_1 + m_a)\alpha + c_1 + G, \qquad a_2 = c_1\alpha + k_1 \\ a_3 = k_1\alpha \end{gathered} \tag{10}$$

The Hurwitz determinant $D_1 \equiv a_1a_2 - a_0a_3$ is positive for arbitrary positive values of G. Furthermore, even when the disturbance force is expressed as the step-function, that is, $F_{d1}(s) \propto 1/s$, the frequency-domain responses do not have singularity stronger than $1/s$ for $s \to 0$ and thus the time-domain responses are bounded, provided that α is positive.

The foregoing discussion is effective for analytically examining the physical reason for the instability, but cannot be extended to multi-degree-of-freedom primary structures because derivation of the characteristic polynomial and the Hurwitz determinants requires very lengthy hand calculations. To avoid this difficulty, the force acting on the primary structure due to the presence of the vibration absorber is calculated from Eq. (2) as

$$\hat{f}_a(t) \equiv c_a\dot{u}_a + k_au_a - f_a = -m_a(\ddot{x}_1 + \ddot{u}_a) \tag{11}$$

Solving the s-domain expression of Eq. (7) for $U_a(s)$ and substituting the resulting solution into the s-domain expression of Eq. (11) leads to

$$\hat{F}_a(s) = -(m_a\alpha + G)[s/(s + \alpha)]sX_1(s) \tag{12}$$

Therefore, the unstable velocity feedback can be transformed into the stable velocity control with high-pass filter $s/(s + \alpha)$ incorporated.

Application Examples

Application to Vibration Control

Consider a mass-spring layered structure as shown in Fig. 2. Such a structure is widely used as a model of a building [8]. The translational motion in the x direction and the rotational motion around the z axis are taken into account in deriving the basic equations and the control law. The equation for the translational motion of the ith layer is given as an example:

$$\begin{aligned} m_i\ddot{x}_i - k_{i+1}x_{i+1} + (k_i + k_{i+1})x_i - k_ix_{i-1} = f_{di} + \delta_{ij}[(k_{a1}u_{a1} \\ + c_{a1}\dot{u}_{a1} - f_{a1}) + (k_{a2}u_{a2} + c_{a2}\dot{u}_{a2} - f_{a2})] \end{aligned} \tag{13}$$

where x_0, θ_0, and $k_{i_{\max}+1}$ are zero and Kronecker's delta means that due to the presence of the driven masses, the jth layer undergoes the force in the bracket.

Because the displacements of the attachment positions of the driven masses are $x_j - l_1\theta_j$ and $x_j + l_2\theta_j$, the equations of motion of the driven masses are

$$\ddot{u}_{an} + 2\zeta_{an}\omega_{an}\dot{u}_{an} + \omega_{an}^2u_{an} = m_{an}^{-1}f_{an} - (\ddot{x}_j - \varepsilon_nl_n\ddot{\theta}_j) \tag{14}$$

where $n = 1, 2$; $\varepsilon_1 = 1$, and $\varepsilon_2 = -1$. Defining absorber masses' general coordinates $v = (l_2u_{a1} + l_1u_{a2})/(l_1 + l_2)$ and $\phi = (u_{a2} - u_{a1})/(l_1 + l_2)$ that are, respectively, assigned to the control of the

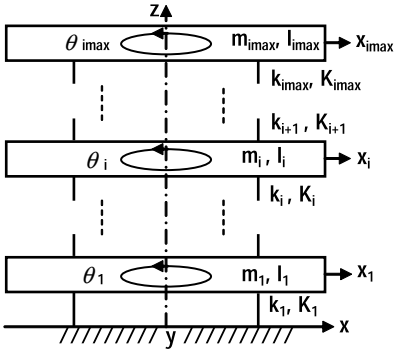

a) Mass-spring layered structure with translational and rotational motions

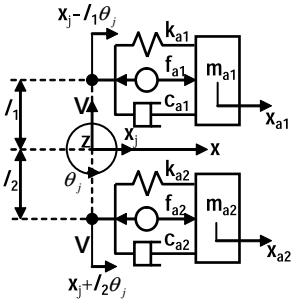

b) Two vibration absorbers attached to the j th layer (the case of $j = i_{\max}$ is considered in this paper)

Fig. 2 Application example.

translational and rotational motions of the primary structure, expressing Eq. (14) in terms of v and ϕ, and eliminating $\ddot{\phi}$ and $\ddot{v}$ from the resulting equations leads to Eqs. (15a) and (15b), respectively:

$$\ddot{v} + (l_1 + l_2)^{-1}[2\zeta_{a1}\omega_{a1}l_2(\dot{v} - l_1\dot{\phi}) + \omega_{a1}^2 l_2(v - l_1\phi) + 2\zeta_{a2}\omega_{a2}l_1(\dot{v} + l_2\dot{\phi}) + \omega_{a2}^2 l_1(v + l_2\phi)] = (l_1 + l_2)^{-1}(m_{a1}^{-1}l_2 f_{a1} + m_{a2}^{-1}l_1 f_{a2}) - \ddot{x}_j \quad (15a)$$

$$\ddot{\phi} - (l_1 + l_2)^{-1}[2\zeta_{a1}\omega_{a1}(\dot{v} - l_1\dot{\phi}) + \omega_{a1}^2(v - l_1\phi) - 2\zeta_{a2}\omega_{a2}(\dot{v} + l_2\dot{\phi}) - \omega_{a2}^2(v + l_2\phi)] = (l_1 + l_2)^{-1}(-m_{a1}^{-1}f_{a1} + m_{a2}^{-1}f_{a2}) - \ddot{\theta}_j \quad (15b)$$

The target absorber equations here are

$$\ddot{v} + \alpha\dot{v} = (l_1 + l_2)^{-1}[m_{a1}^{-1}l_2 G(\dot{x}_j - l_1\dot{\theta}_j) + m_{a2}^{-1}l_1 G(\dot{x}_j + l_2\dot{\theta}_j)] - \ddot{x}_j \quad (16a)$$

$$\ddot{\phi} + \alpha\dot{\phi} = (l_1 + l_2)^{-1}[-m_{a1}^{-1}G(\dot{x}_j - l_1\dot{\theta}_j) + m_{a2}^{-1}G(\dot{x}_j + l_2\dot{\theta}_j)] - \ddot{\theta}_j \quad (16b)$$

where $\dot{x}_j - l_1\dot{\theta}_j$ and $\dot{x}_j + l_2\dot{\theta}_j$ are the velocities of the attachment positions of the absorbers. By forcing the residual between Eqs. (15a) and (16a) and that between Eqs. (15b) and (16b) to be zero, the two driving forces can be determined as

$$f_{a1} = G(\dot{x}_j - l_1\dot{\theta}_j) + m_{a1}[\omega_{a1}^2 v + (2\zeta_{a1}\omega_{a1} - \alpha)\dot{v} - \omega_{a1}^2 l_1\phi + (\alpha - 2\zeta_{a1}\omega_{a1})l_1\dot{\phi}] \quad (17a)$$

$$f_{a2} = G(\dot{x}_j + l_2\dot{\theta}_j) + m_{a2}[\omega_{a2}^2 v + (2\zeta_{a2}\omega_{a2} - \alpha)\dot{v} + \omega_{a2}^2 l_2\phi + (2\zeta_{a2}\omega_{a2} - \alpha)l_2\dot{\phi}] \quad (17b)$$

The terms in the brackets can be computed, once v and ϕ are determined using the detected values of u_{a1} and u_{a2}.

Numerical results are presented in Fig. 3. The parameters of the primary structure are presented in Table 1 whereas the parameters of the vibration absorbers are as follows:

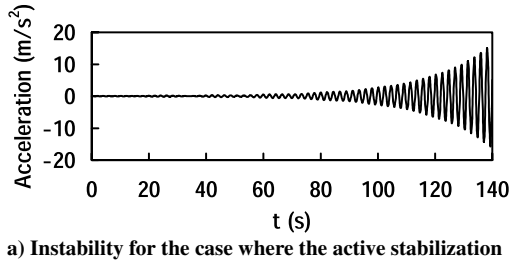

a) Instability for the case where the active stabilization is not present (G =80 Ns/m, $\omega / 2\pi$ =0.5Hz)

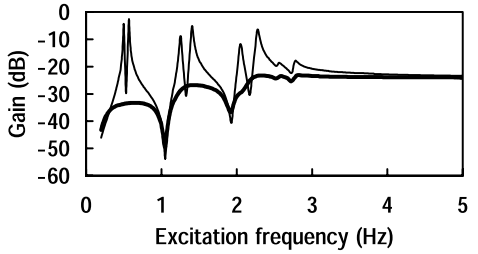

b) Control performance for the case where the active stabilization is applied (G =2000 Ns/m, α =0.48π s^{-1}; ——, controlled; ——, uncontrolled)

Fig. 3 Responses of acceleration $\ddot{x}_{i_{\max}} + l_2\ddot{\theta}_{i_{\max}}$ of the structure shown in Fig. 2 ($i_{\max} = 6$).

Table 1 Parameters of the mass-spring layered structure shown in Fig. 2

i	Translation		Rotation	
	m_i, kg	k_i, N/m	I_i, kg · m^2	K_i, Nm/rad
1	354.2	159,100	236.3	123,900
2	354.2	93,270	236.3	72,610
3	354.2	50,350	236.3	39,200
4	354.2	50,350	236.3	39,200
5	354.2	24,280	236.3	18,900
6	393.6	24,280	207.4	18,900

$$m_{a1} = m_{a2} = 15 \text{ kg}, \qquad \zeta_{a1} = \zeta_{a2} = 0.1$$
$$\omega_{a1} = \omega_{a2} = 3.14 \text{ rad/d}, \qquad l_1 = l_2 = 0.75 \text{ m}$$

A modal damping ratio 0.01 is introduced to each mode of the primary structure and the response of $\ddot{x}_{i_{\max}} + l_2\ddot{\theta}_{i_{\max}}$ to the excitation $f_{di_{\max}} = m_{di_{\max}} = 10 \sin \omega t$ is shown. When the active stabilization is not present and only the velocity feedback terms in Eq. (17) are applied, the system exhibits instability even for a small value of the control gain G, as is illustrated in Fig. 3a. To avoid this instability, the active stabilization was applied and the frequency response under a high control gain was calculated by repeating the time response analysis to compute the stationary amplitude for each excitation frequency. The result is shown in Fig. 3b, in which effective control performance can be confirmed.

Figure 4 shows dependence of the control performance on variation in the primary structure for the first mode of the translational motion (Fig. 4a) and the first mode of the rotational motion (Fig. 4b). The control performance is represented by the real part of the eigenvalue of the controlled system for each mode, whereas the variation in the primary structure is represented by the ratio between the varying and the original eigenfrequencies of the uncontrolled system. The variation in each mode's eigenfrequency is given by varying the mass and the inertia moment of each layer. For the sake of comparison, results in a past work [8] for the cases where $H\infty$ and μ synthesis control methods were applied are presented. In these cases, as is pointed out also in the work, the real part of the eigenvalue for each mode increases and the system becomes unstable when the variation in the primary structure increases. Thus, it can be confirmed from Fig. 4 that model independence of the control performance is improved through the active stabilization method.

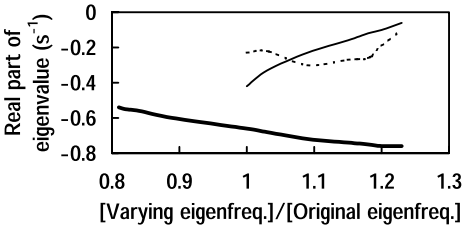

a) The first translational mode

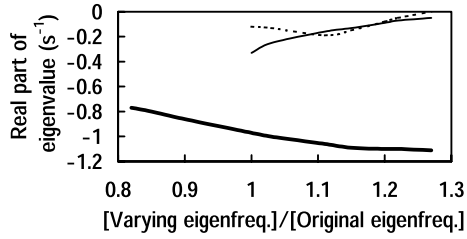

b) The first rotational mode

Fig. 4 Dependence of control performance on variation in the primary structure (bold line, present active stabilization; dashed line, $H\infty$ control [8]; solid line, μ synthesis [8]).

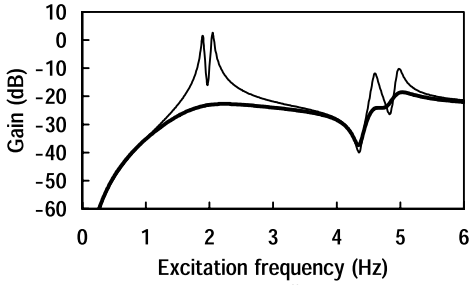

Fig. 5 Frequency responses of $\ddot{x}_{i_{\max}} + l_2\ddot{\theta}_{i_{\max}}$ of the structure shown in Fig. 2 ($i_{\max} = 2$; illustration of robustness against variation in the primary structure; bold line, controlled; solid line, uncontrolled).

If we use the control methods whose model independence is not so strong, we encounter a problem that parameters of the controller must be frequently altered for marked variations in a primary structure. A typical example is a building under construction, whose modal parameters markedly vary with the change in the number of layers. Relief of controller designers from this problem is the motivation of this study. As a check, the same control that brought about the result in Fig. 3b was applied to the cases of $i_{\max} = 1$–5 without any change in the parameters of the controller and it was confirmed that the control was still stable and effective. An illustrative result for these cases is presented in Fig. 5.

The present method is robust against variations in a primary structure because it transforms the unstable controller into a stable controller. Then, how about robustness against parameter identification errors for a vibration absorber system. This robustness is illustrated in Fig. 6, in which the case of $\zeta_{a1} = \zeta_{a2} = \zeta_a$, $\omega_{a1} = \omega_{a2} = \omega_a$, and $m_{a1} = m_{a2} = m_a$ is considered and the real value of the quantity A is represented by $(A)_{\text{real}}$. The reason for this robustness can be explained as follows. By replacing the estimated values in Eq. (15) by the corresponding real values and substituting Eq. (17) into the resulting equations, we obtain the equations for the actually implemented controllers as

$$\ddot{v} + [\alpha + 2(\zeta_a\omega_a)_{\text{real}} - 2\zeta_a\omega_a]\dot{v} + [(\omega_a^2)_{\text{real}} - \omega_a^2]v = m_a^{-1}G\dot{x}_j - \ddot{x}_j \tag{18a}$$

$$\ddot{\phi} + [\alpha + 2(\zeta_a\omega_a)_{\text{real}} - 2\zeta_a\omega_a]\dot{\phi} + [(\omega_a^2)_{\text{real}} - \omega_a^2]\phi = m_a^{-1}G\dot{\theta}_j - \ddot{\theta}_j \tag{18b}$$

The coefficient of $\dot{v}$ and $\dot{\phi}$ is the cutoff frequency of the high-pass filter as is discussed for Eq. (12). Let us set its admissible range as

$$0.1(\omega_a)_{\text{real}} < \alpha + 2(\zeta_a\omega_a)_{\text{real}} - 2\zeta_a\omega_a < 0.8(\omega_a)_{\text{real}} \tag{19}$$

Substituting $\alpha/\omega_a = 0.5$ and $\zeta_a = 0.1$ as the example values used for Fig. 3b transforms the inequality (19) into

$$0.05 - 0.15\omega_a/(\omega_a)_{\text{real}} < (\zeta_a)_{\text{real}} < 0.4\text{–}0.15\omega_a/(\omega_a)_{\text{real}} \tag{20}$$

Most real vibration absorbers satisfy this condition if ω_a is selected such that $0.9 \le \omega_a/(\omega_a)_{\text{real}} \le 1$. Therefore, the control performance is not seriously affected by a damping ratio identification error. Furthermore, it can be seen from the coefficient of v and ϕ in Eq. (18) that overestimation of the eigenfrequency of the vibration absorber is prohibited but underestimation of it within 10% does not cause a serious problem. Thus, robustness can be estimated and achieved effectively by using vibration absorber equations without using governing equations for primary structures.

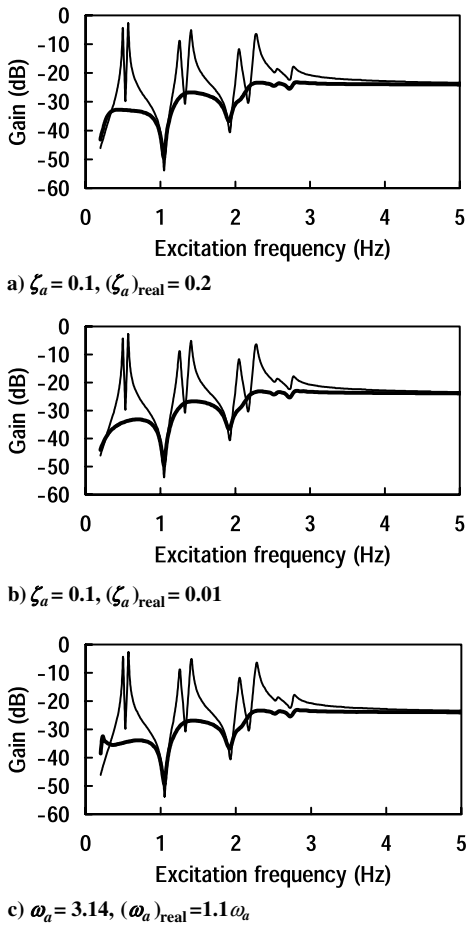

Fig. 6 Frequency responses of $\ddot{x}_{i_{\max}} + l_2\ddot{\theta}_{i_{\max}}$ of the structure shown in Fig. 2 ($i_{\max} = 6$; robustness against parameter identification errors for the vibration absorbers; bold line, controlled; solid line, uncontrolled).

Application to Vibration Isolation

This active stabilization method serves as a solution method to the vibration isolation problem when skyhook damping requiring that a damper be connected to an inertial reference frame is not practical as in most situations. A beam-model subjected to a base excitation x_b as shown in Fig. 7 is considered as an example and frequency responses of the acceleration $\ddot{x}_1$ are shown in Fig. 8. In this example, the beam has a density of 7, 850 kg/m^3, length of 1.5 m, thickness of 0.002 m, width of 0.05 m, and Young's modulus of 2×10^{11} N/m^2; the parameters of the vibration absorber are $m_a = 0.03$ kg, $\zeta_a = 0.1$, and $\omega_a = 7.54$ rad/s; the damping and spring constants of the support are $c_b = 0.005$ Ns/m and $k_b = 16$ N/m; the base excitation amplitude is 0.001 m. A modal damping ratio of 0.01 is introduced to each vibration mode of the beam. Figure 8a illustrates the well-known problem that the response of $\ddot{x}_1$ is increased for high frequencies when the damping constant c_b is increased. As shown in Fig. 8b, this problem can be solved by attaching the hybrid vibration absorber and applying the active stabilization method.

Figure 9 shows the magnitude of the driving force required for achieving the vibration isolation performance shown in Fig. 8b. The result for the full active case with $\omega_a = 0$ is presented for the sake of comparison. It can be seen from Fig. 9 that by using the active stabilization method, the large magnitude reduction of the driving force is achieved near the first resonant frequency of the primary structure. The magnitude of the driving force increases when the excitation frequency ω tends to zero; however, this tendency can be

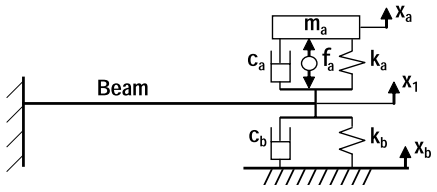

Fig. 7 Vibration isolation problem for a beam.

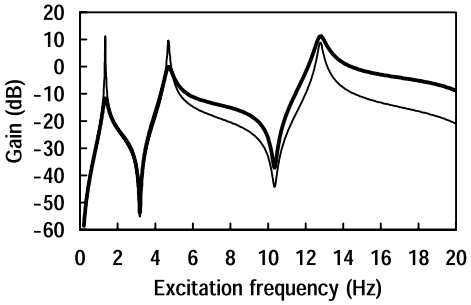

a) Uncontrolled case where the vibration absorber is not present (——— , c_b = 0.005 Ns/m; ———, c_b = 0. 5 Ns/m)

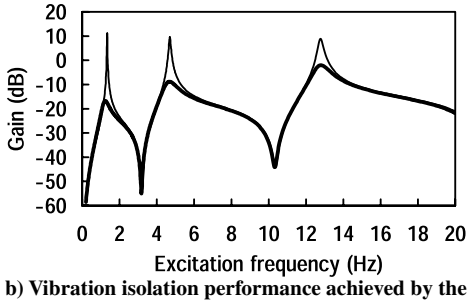

b) Vibration isolation performance achieved by the active stabilization (c_b =0.005 Ns/m; ———, controlled with G =1 Ns/m and α =1.6π s^{-1} ;———, uncontrolled)

Fig. 8 Frequency responses of $\ddot{x}_1$ of the beam shown in Fig. 7.

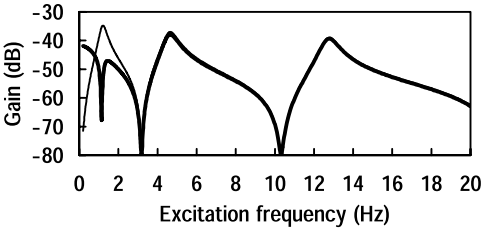

Fig. 9 Frequency responses of the driving force f_a(bold line, active stabilization of hybrid absorber; solid line, full active case).

controlled by selecting the damping constant of the target absorber equation as a not-so-small value to assure the stability as is explained for Eq. (9). Therefore, the magnitude of the driving force for $\omega \to 0$ is well smaller than the maximal magnitude for the full active case at the first resonant frequency of the primary structure. Thus, the present active stabilization method is effective for saving power consumption, which is proportional to the square of the magnitude of the driving force, except for the case in which dominant frequencies of excitation are confined within a frequency range well below the first resonant frequency. The reason for this power saving can be explained as follows: Eliminating $U_a(s)$ from the s-domain expressions of Eqs. (7) and (8) leads to the following relation between the driving force and the primary structure's response in the s domain:

$$F_a(s) = \{G(1/s)(s^2 + 2\zeta_a\omega_a s + \omega_a^2) - m_a[(2\zeta_a\omega_a - \alpha)s + \omega_a^2]\}[1/(s+\alpha)]s^2X_1(s) \tag{21}$$

The braced quantity is dominated by its leading term under the high-gain control. This term includes the factor exactly the same as the characteristic polynomial of the hybrid vibration absorber, whose magnitude is small near the eigenfrequency of the hybrid vibration absorber.

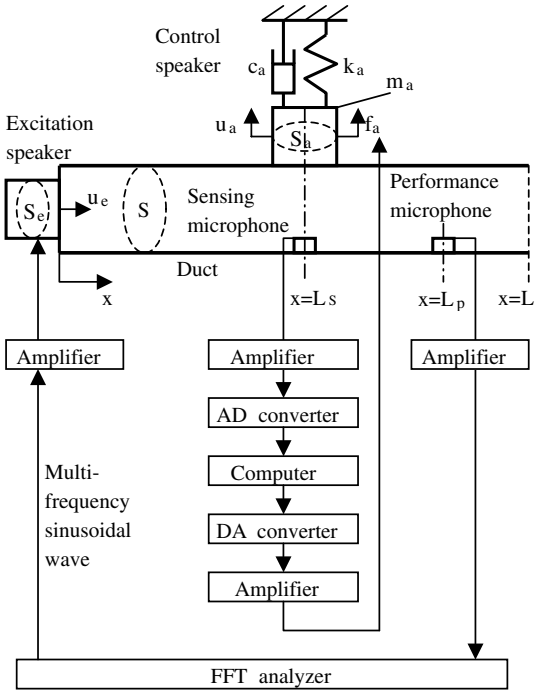

Fig. 10 Experimental setup of active noise control for duct.

Application to Active Noise Control

The present active stabilization method can be extended to the active noise control problem by considering a control speaker (actuator) a hybrid vibration absorber coupled with a sound field to be controlled, as is outlined in the Appendix. An experimental study is conducted by using a system shown in Fig. 10. The parameters of the system are as follows:

$$L = 1 \text{ m}, \quad L_s = 0.5 \text{ m}, \quad L_p = 0.8 \text{ m}; \quad S = 0.044^2 \text{ m}^2$$
$$S_e/S = S_a/S = 0.365; \quad \alpha = 40 \text{ s}^{-1}, \quad G = 0.004 \text{ Ns/m}$$
$$m_a = 0.00176 \text{ kg}, \quad \zeta_a = 0.1, \quad \omega_a/2\pi = 140 \text{ Hz}$$

The driven mass m_a of the control speaker was measured directly and the damping ratio ζ_a and the eigenfrequency ω_a were estimated by measuring the frequency response of the acceleration of the driven mass to an excitation force. The digital sampling frequency was set to be 50,000 Hz.

Figure 11 shows a measured transfer function from the acceleration of the excitation speaker to the sound pressure at the performance microphone. The excitation signal is a multifrequency sinusoidal function produced by a FFT analyzer. For the sake of comparison, the measured transfer function for the uncontrolled case where the control speaker is removed and the resulting hole is covered by a rigid wall is shown using a dotted line. The effectiveness of the active stabilization method in suppressing

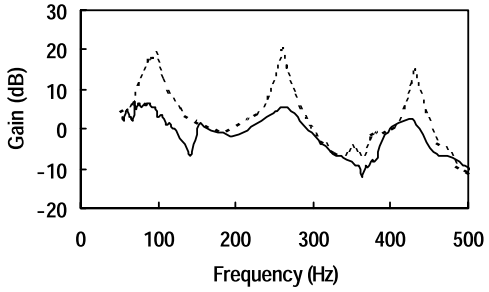

Fig. 11 Experimental results (solid line, controlled; dashedl line, uncontrolled).

acoustic modes can be confirmed. Furthermore, a sharp valley is observed at the eigenfrequency of the control speaker. This valley indicates that the control speaker works as a hybrid vibration absorber coupled with the sound field.

It is known that if a sensing microphone is located near a control speaker, the direct field of the control speaker may dominate the sound field to be detected and destabilize the control system. This phenomenon can be controlled to some extent in the present active stabilization method, because the magnitude of the controller transfer function is small near the eigenfrequency of the control speaker, as can be seen from Eq. (A8). Furthermore, it was found through the experiment that this phenomenon can be controlled by inserting sound-absorbing material between the sensing microphone and the duct wall opposite to the control speaker, only within a short longitudinal interval near the sensing microphone. The reason for this can be considered as follows: When the sound-absorbing material is not present, the direct field is subjected to the boundary condition that requires the sound pressure be maximal at the rigid wall. This boundary condition can be relaxed by the sound-absorbing material. When the sound-absorbing material is not present, the achieved reduction of the sound pressure level for the first–third modes in Fig. 11 is reduced to 8, 5, and 4 dB, respectively. However, even in this case, the effect of this active control can be appreciated especially for lower frequencies, where the importance of active control technologies is accentuated due to poor control performance of passive methods.

Conclusions

A method of actively stabilizing a hybrid vibration absorber driven by a force proportional to the velocity detected at the attachment position of the absorber has been studied as a means to improve model independence of robust performance while allowing for multimode controllability for the case in which a hybrid vibration absorber is desired as an actuator. Robustness also against parameter identification errors in a vibration absorber system was discussed and illustrated by an application example. It was illustrated that the present active stabilization method is effective for saving power consumption, except for the case in which low dominant frequencies of excitation are confined within a frequency range well below the first resonant frequency of a primary structure. This active stabilization method serves as a means to solve the vibration isolation problem, when skyhook damping, which requires that a damper be connected to an inertial reference frame, is not practical as in most situations. This method can be applied to the active noise control problem, because a control speaker can be modeled as a hybrid vibration absorber coupled to a sound field to be controlled and its relatively high eigenfrequency lies in the bandwidth where control is desired. Regarding the active noise control problem, an experimental result was presented.

Appendix: Extension to Active Noise Control Problem

The wave equation for the system shown in Fig. 10 is

$$\partial^2 p/\partial t^2 - c^2 \partial^2 p/\partial x^2 = (\rho_0 c^2/S)[S_e \ddot{u}_e \delta(x) - S_a \ddot{u}_a \delta(x - L_s)] \tag{A1}$$

The right-hand side of Eq. (A1) represents the time derivative of the volume source per unit volume. By expressing the sound pressure in terms of the modal function as $p(x,t) = \sum_{n=1}^{n_{\max}} q_n(t) X_n(x)$, where $X_n(x) = \cos[(2n-1)\pi x/2L]$, and introducing the modal damping ratio ζ_n, Eq. (A1) can be transformed into the modal equation:

$$\ddot{q}_n + 2\zeta_n \omega_n \dot{q}_n + \omega_n^2 q_n = (2\rho_0 c^2/L)[(S_e/S)\ddot{u}_e X_n(0) - (S_a/S)\ddot{u}_a X_n(L_S)] \tag{A2}$$

The equation of motion of the actuator subject to the driving force $f_a(t)$ is

$$m_a(\ddot{u}_a + 2\zeta_a \omega_a \dot{u}_a + \omega_a^2 u_a) = S_a p(L_s, t) + f_a(t) \tag{A3}$$

When the driving force is determined as $f_a(t) = S_a G\, \mathrm{d}p(L_s,t)/\mathrm{d}t$ ($G > 0$), the characteristic equation for Eq. (A2) with $n = 1$ and Eq. (A3) can be derived as

$$a_0 s^4 + a_1 s^3 + a_2 s^2 + a_3 s + a_4 = 0 \tag{A4}$$

where

$$\begin{gathered} a_0 = 1 \\ a_1 = 2\zeta_a \omega_a + 2\zeta_1 \omega_1 + (2\rho_0 c^2/Lm_a)(S_a^2/S)X_1^2(L_s)G \\ a_2 = \omega_a^2 + 4\zeta_1 \omega_1 \zeta_a \omega_a + \omega_1^2 + (2\rho_0 c^2/Lm_a)(S_a^2/S)X_1^2(L_s) \\ a_3 = 2\zeta_1 \omega_1 \omega_a^2 + 2\zeta_a \omega_a \omega_1^2, \qquad a_4 = \omega_1^2 \omega_a^2 \end{gathered} \tag{A5}$$

The stability conditions expressed in terms of the Hurwitz determinants are $D_1 \equiv a_1 a_2 - a_0 a_3 > 0$ and $D_2 \equiv a_3 D_1 - a_4 a_1^2 > 0$. Because a_1 increases linearly with G, the second stability condition does not admit the infinite increase of the gain G. To solve this problem, the driving force is determined as

$$f_a = m_a[(2\zeta_a \omega_a - \alpha)\dot{u}_a + \omega_a^2 u_a] + S_a G\, \mathrm{d}p(L_s,t)/\mathrm{d}t \tag{A6}$$

such that Eq. (A3) coincides with the following target equation:

$$m_a(\ddot{u}_a + \alpha \dot{u}_a) = S_a p(L_s,t) + S_a G\, \mathrm{d}p(L_s,t)/\mathrm{d}t \tag{A7}$$

To make this control law (A6) implementable only through the sensing of the sound pressure, we eliminate $U_a(s)$ from the Laplace transforms of Eqs. (A6) and (A7), thereby determining the controller transfer function:

$$H(s) \equiv \frac{F_a(s)}{P(L_s,s)} = \frac{S_a}{s+\alpha}\left[G(s^2 + 2\zeta_a \omega_a s + \omega_a^2) + \frac{(2\zeta_a \omega_a - \alpha)s + \omega_a^2}{s}\right] \tag{A8}$$

References

[1] Yuan, J., "Hybrid Vibration Absorber by Zero/Pole-Assignment," *Journal of Vibration and Acoustics*, Vol. 122, Oct. 2000, pp. 466–469.

[2] Olgac, N., Elmali, H., Hosek, M., and Renzulli, M., "Active Vibration Control of Distributed Systems Using Delayed Resonator with Acceleration Feedback," *Journal of Dynamic Systems, Measurement, and Control*, Vol. 119, Sept. 1997, pp. 380–389.

[3] Jalili, N., and Olgac, N., "A Sensitivity Study on Optimum Delayed Feedback Vibration Absorber," *Journal of Dynamic Systems, Measurement, and Control*, Vol. 122, June 2000, pp. 314–321.

[4] Filipovic, D., and Schroder, D., "Bandpass Vibration Absorbers," *Journal of Sound and Vibration*, Vol. 214, No. 3, 1998, pp. 553–566.

[5] Seto, K., and Mitsuda, S., "A New Method for Making a Reduced-Order Model of Flexible Structures Using Unobservability and Uncontrollability and Its Application in Vibration Control," *JSME International Journal*, Vol. 37, No. 3, 1994, pp. 444–449.

[6] Bruner, A. M., Belvin, W. K., Horta, L. G., and Juang, J. N., "Active Vibration Absorber for the CSI Evolutionary Model: Design and Experimental Results," *Journal of Guidance, Control, and Dynamics*, Vol. 15, No. 5, 1992, pp. 1253–1257.

[7] Nonami, K., Nishimura, H., and Tian, H., "H∞/μ Control-Based Frequency-Shaped Sliding Mode Control for Flexible Structures," *JSME International Journal*, Vol. 39, No. 3, 1996, pp. 493–501.

[8] Koike, Y., Nonami, K., Nishimura, H., Sazuka, H., Tanida, K., and Suzuki, T., "Bending-Torsional Vibration Control of Flexible Structure by Using a Pair of Hybrid Mass Damper Based on H∞/μ Control Theory," JSME Paper 95-28, 1995, pp. 209–212.

[9] Burdisso, R. A., and Heilmann, J. D., "A New Dual-Reaction Mass Dynamic Vibration Absorber Actuator for Active Vibration Control," *Journal of Sound and Vibration*, Vol. 214, No. 5, 1998, pp. 817–831.

[10] von Flotow, A. H., Beard, A., and Bailey, D., "Adaptive Tuned Vibration Absorbers: Tuning Laws, Tracking Agility, Sizing and Physical Implementations," *Proceedings of NOISE-CON, 94*, Vol. 1, Ft. Lauderdale, FL, 1994, pp. 437–454.

[11] Franchek, M. A., Ryan, M. W., and Bernhard, R. J., "Adaptive Passive Vibration Control," *Journal of Sound and Vibration*, Vol. 189, No. 5,

1995, pp. 565–585.
[12] Morgan, R. A., and Wang, K. W., "An Active-Passive Piezoelastic Absorber for Structural Vibration Control Under Harmonic Excitations With Time-Varying Frequency, Part 1: Algorithm Development and Analysis," *Journal of Vibration and Acoustics*, Vol. 124, Jan. 2002, pp. 77–83.
[13] Davis, C. L., and Lesieutre, G. A., "An Actively Tuned Solid-State Vibration Absorber Using Capacitive Shunting of Piezoelastic Stiffness," *Journal of Sound and Vibration*, Vol. 232, No. 3, 2000, pp. 601–617.

C. Pierre
Associate Editor